Scanning Microscopy

Volume 2 | Number 1 Article 4

10-19-1987

3-Dimensional Imaging of Biological Structures by High Resolution Confocal Scanning Laser Microscopy

G. J. Brakenhoff
University of Amsterdam

H. T. M. van der Voort
University of Amsterdam

E. A. van Spronsen
University of Amsterdam

N. Nanninga
University of Amsterdam

Scanning Microscopy, Vol. 2, No. 1, 1988 (Pages 33-40) 0891-7035/88$3.00+.00
Scanning Microscopy International, Chicago (AMF O'Hare), IL 60666 USA

3-DIMENSIONAL IMAGING OF BIOLOGICAL STRUCTURES BY HIGH RESOLUTION CONFOCAL SCANNING LASER MICROSCOPY

G.J. Brakenhoff*, H.T.M. van der Voort, E.A. van Spronsen and N. Nanninga

Department of Electron Microscopy and Molecular Cytology, University of Amsterdam,
Plantage Muidergracht 14, 1018 TV Amsterdam, The Netherlands

(Received for publication March 04, 1987, and in revised form October 19, 1987)

Abstract

Imaging in confocal microscopy is characterized by the ability to make a selective image of just one plane inside a specimen, virtually unaffected -within certain limits- by the out-of-focus regions above and below it. This property, called optical sectioning, is accompanied by improved imaging transverse to the optical axis. We have coupled a confocal microscope to a computer system, making the combination of both an excellent instrument for mapping the 3-dimensional structure of extended specimens into a computer memory/data array. We measured that the volume element contributing to each data point has, under typical fluorescence conditions, a size of 0.2 x 0.2 x 0.72 μm. The data can be analysed and represented in various ways, i.e., stereoscopical views from any desired angle. After a description of the experimental arrangement, we show various examples of biological and food-structural studies. The microscope can be operated either in reflection or in fluorescence. In the latter mode a spectral element allows selection of the wavelength band of fluorescence light contributing to the image. In this way, we can distinguish various structures inside the cell and study their 3-dimensional relationships. Various applications in biology and the study of food structure are presented.

Key words: 3-dimensional, confocal, light microscopy, fluorescence, reflection microscopy, laser microscopy

* Address for correspondence:
G.J. Brakenhoff
Dept. of Electron Microscopy & Molecular Cytology
University of Amsterdam
Plantage Muidergracht 14, 1018 TV Amsterdam
The Netherlands
Phone No. (31)20-5255187

Introduction

Confocal scanning light microscopy forms a bridge between conventional light microscopy with its limited resolution (but capable of imaging hydrated, possibly live, specimen) on one side, and electron microscopy with its higher resolution on the other. One of the main drawbacks of electron microscopy is that the various specimen-preparation techniques such as chemical fixation, dehydration and sectioning, may affect the apparent morphology. For instance, a volume shrinkage of up to 50% has been observed in bacteria as a consequence of such preparation steps (Woldringh et al., 1976). Light microscopy on the other hand, permits the observation of the biological specimen in a hydrated or live condition, however, with limited resolution. Confocal microscopy now offers not only an effective increase in imaging capabilities, but also (when coupled to a computer/image processing system) vastly increased possibilities for specimen analysis and presentation.

The basic confocal principle has been described by Sheppard and Choudhury (1977) and an early demonstration of the imaging capabilities was given by Brakenhoff et al. (1979, 1981). The first applications connected with the optical sectioning property on biological material were reported by Brakenhoff et al. (1985), Van der Voort et al. (1985), Wijnaendts van Resandt (1985), Carlsson et al. (1985) and Petran et al. (1985). The latter uses an instrument in which, with the help of Nipkov disks, sectioning properties are realized.

The confocal microscope

The basic arrangement of the instrument for reflection/fluorescence operation is presented in Fig. 1. Characteristic for confocal microscopy is that the same point in the specimen is both optimally illuminated as well as optimally imaged on a point detector. When diffraction-limited optics are employed, it can be shown that at a given Numerical Aperture (N.A.) the point response of a confocal system will be narrower by a factor of 1.4 (Sheppard and Choudhury, 1977; Brakenhoff et al., 1979). This so-called confocal effect is associated with the fact that the response

function in confocal microscopy can be described as the product of the illumination distribution and the detection sensitivity distribution. The latter is defined by the back-projected image of the detection pinhole in the object plane. In order to profit from this improvement in imaging characteristics, it is necessary to employ optics with maximum possible N.A., i.e., immersion optics with an N.A. of 1.3 to 1.4. Only then an absolute gain with respect to conventional microscopy can be realized. It has been shown (Brakenhoff et al., 1979, 1981) that the expected improvement could indeed be realized with high N.A. optics resulting in effective point responses with widths at half intensity down to 130 to 140 nm in transmission confocal microscopy. This narrowing of the point response takes place in 3 dimensions, thus reducing the volume of the specimen contributing to an image element by a factor of $(1.4)^3 \approx 3$. A comparable increase in the amount of information to be extracted from the specimen results.

The confocal principle also holds in fluorescence with a few modifications. The main ones are the incoherence of the excited fluorescence radiation, which affects the imaging positively (Cox et al., 1982) and the finite size of the detection pinhole, which has a negative influence. A somewhat larger pinhole than desirable from the confocal point of view is often necessary in fluorescence to get a sufficiently high signal-to-noise ratio in the collected signal.

An aspect implicit in the confocal principle, which deserves special attention is the sectioning property. In normal microscopy all the radiation generated at the various levels in the specimen reaches the image plane, causing a (often strong) reduction of the contrast of the image of the in-focus part of the specimen. In confocal microscopy the detection pinhole used, together with the effect of the illumination precisely focussed on the specimen point imaged, will suppress quite effectively the out-of-focus contributions. Thus an image is produced which is only related to the in-focus specimen plane. The best conceptual illustration of this confocal sectioning property is that in normal microscopy one cannot determine the vertical position level in a specimen of a uniform thin layer of fluorescent material: the light intensity reaching the image plane is independent of the axial position of this layer. In confocal microscopy one can determine the position of this uniform layer with the accuracy as defined by its improved response function.

The microscope reported about here is based on mechanical scanning of the specimen through the confocal point. This approach, which is called "on-axis scanning" as the lens is used to image just one point on the axis, has several advantages over situations where scanning is effected by sweeping the beam over the specimen (off-axis scanning). The main ones are: (i) The lens is used in the best corrected image field avoiding off-axis aberrations. (ii) The field of view to be imaged by the microscope is not limited by the optics but by the scan amplitude of the mechanical scan, which can be up to several millimeters. (iii) The imaging characteristics for each point of the scanned specimen are identical, a property

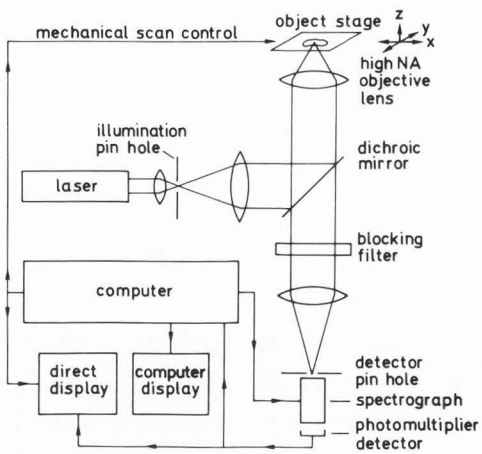

Fig. 1. Schematic diagram of the confocal scanning microscope for the fluorescence and reflection mode of operation. Light originating from the laser-illuminated pinhole is focussed on a certain point of the specimen. This point is subsequently imaged on the detector pinhole. The technique is called confocal since the image of the illumination pinhole and the back-projection of the detector pinhole have a common focus in the specimen. The specimen is scanned mechanically through the confocal point and a direct image is created on a display modulated by the detected intensity, running in synchrony with the mechanical scan. In addition, the image data are stored in the computer system and are first used to generate a continuous viewing image, independent of the mechanical scan. After data collection, various types of 2-D and 3-D image processing routines are available (see below). The optical set-up dichroic mirror/blocking filter is the standard arrangement in fluorescence microscopy. With the spectrograph we can select a certain band from the fluorescence radiation for image formation. For operation in reflection, the dichroic mirror is replaced by a 50% beamsplitter mirror, the blocking filter is removed and the spectrograph tuned to the desired wavelength. Both the wavelength selection as well as the band width of the spectrograph can be set by the computer system.

especially important in view of subsequent image processing and analysis. Our instrument and the one operated by Wijnaendts van Resandt (1985) are of the on-axis type while those of Carlsson et al. (1985) and Petran et al. (1985) are of the off-axis type.

Instrumentation

The instrument as illustrated in Fig. 1 consists basically of a scanning unit, the confocal optical arrangement and a computer system for controlling the instrument, collecting data and providing the image processing facilities.

The key element in a scanning microscope is the stability and the repeatability of the mechanical scan movement. In order not to affect the performance of the microscope, this scan movement should

be controlled considerably better than the expected optical resolutions of 100-200 nm. We were able to attain an accuracy of better than 20 nm in an approach detailed in Marsman et al. (1983). The table is scanned in a plane transverse to the optical axis with a fast sinus type movement in one direction and a slow stepping type movement in the other. A typical scanning frequency was 50Hz with amplitude up to 1 mm. Higher frequencies up to 300 Hz are possible, though at reduced amplitude. The desired number of lines/image determines the image repetition frequency. A stable viewing image, independent of the mechanical scan, is provided from the frame store (see below) for image evaluation. The low scan frequencies have not been found to be a serious limitation, as the signal to noise ratio in the often somewhat weak fluorescence images would make faster scan rates undesirable. An analogy with SEM operation is applicable: although there fast (up to TV) scan rates are possible, often for the same reasons much lower scan rates are used. No deformation or other effects have been observed in the specimen examined thus far, which were related to acceleration forces associated with the mechanical scanning. This is as expected, since most objects are rather small and mostly embedded in a medium of approximately the same specific gravity as the object itself, and thus no stresses on the object with respect to its direct surroundings result.

The scanning table, together with the confocal optics, are mounted on a vertically oriented optical bench. We have opted for an "inverse" optical system in order to have free accessibility of the specimen during imaging. To realize maximum resolution, we use a high N.A. oil immersion lens with an N.A. of 1.3. This means that in between the scanning specimen, supported on an appropriate glass slide, and the stationary high N.A. lens, a thin layer of immersion oil is present. The choice of laser wavelength to be used is determined by factors like the resolution desired or the fluorescence exitation requirements of the object or its scattering properties. We have presently available a Krypton-Ion laser system with a choice of wavelengths between 337 nm and 650 nm. Beam powers required for successful operation are of the order of 10-50 mWatt with 0.5 to 5 mmW passing the illumination pinhole.

The instrument contains two computers, one small, relatively slow 8-bit system which takes care of the various instrument control functions, and a faster 16-bit type with 68000 processor dedicated to image collection, processing and display functions. This latter system is also used to update the framestore from which the constant 60 Hz repetition rate viewing image is generated. For further details on the organization of the system see Van der Voort et al. (1985). A very useful program written for the instrument control acquires automatically a set of images at specific heights in the specimen according to the parameters set by the operator. The data from this 3-D mapping are put on disk and are the starting material for various image processing applications. We have the standard image processing algorithms available: contrast stretching, contrast inversion, Gaussian and median filtering, local contrast enhancement, etc. In addition to these we have written an algorithm for the generation of stereoscopic image pairs (Van der Voort et al., 1985). As summarized in Fig. 2, the maximum value along a viewing line is assigned to the resulting image. However, alternatives can be chosen. One can, for instance, assign the minimum value or just take a summation of values along the

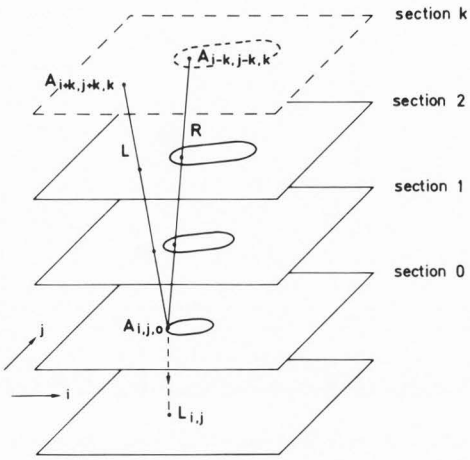

Fig. 2. Stereoscopic image pairs are generated by an algorithm in which we assign the maximum of the pixel values encountered along a viewing line L or R to the corresponding stereoscopic image pair, i.e., a pixel value $L_{i,j}$(i, j : 0..255) will be the maximum of the set of pixel values $A_{i + s_1 k,\ j + s_2 k,\ k}$ (k:0...N-1; N is the number of optical sections. $A_{i,\ j,\ k}$ denotes a pixel of optical section k with coordinates i, j.

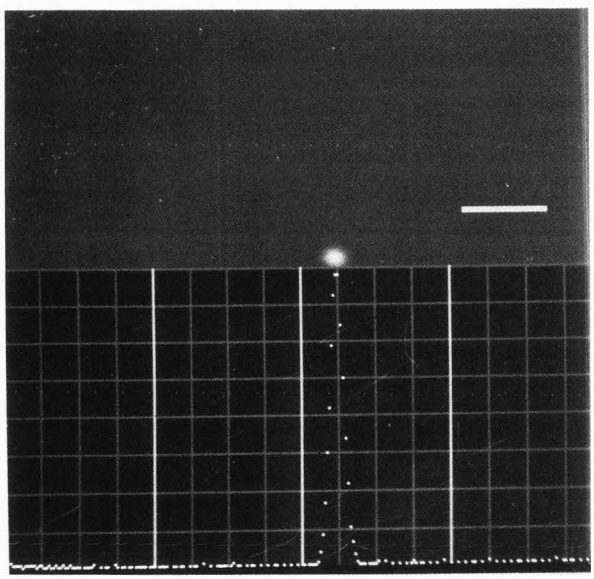

Fig. 3. CSLM image of a small bead (size 50 μm) in reflection, taken at a wavelength of 476 nm with N.A. = 1.3 optics. The plot at half height through the center of the image indicates a response with a width of 190 nm. Bar = 1 μm.

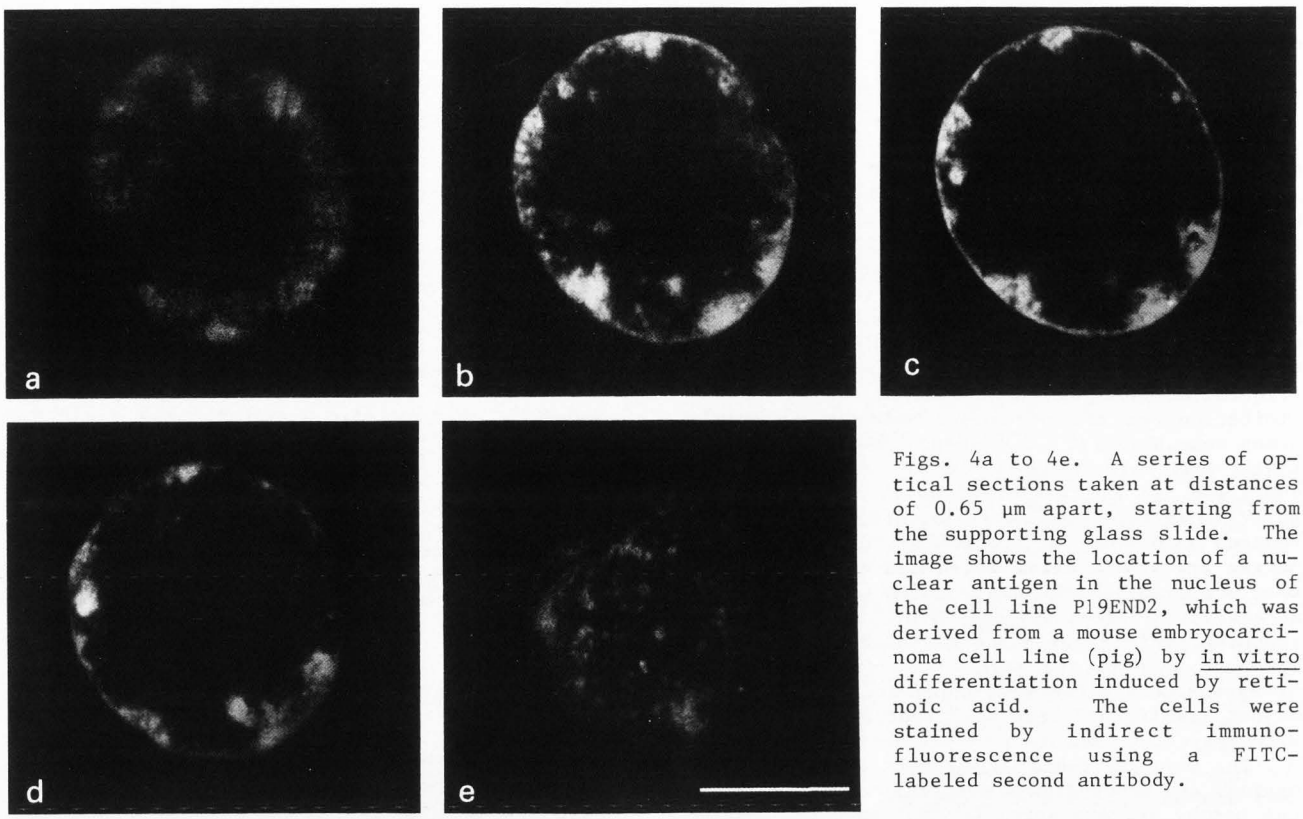

Figs. 4a to 4e. A series of optical sections taken at distances of 0.65 µm apart, starting from the supporting glass slide. The image shows the location of a nuclear antigen in the nucleus of the cell line P19END2, which was derived from a mouse embryocarcinoma cell line (pig) by in vitro differentiation induced by retinoic acid. The cells were stained by indirect immunofluorescence using a FITC-labeled second antibody.

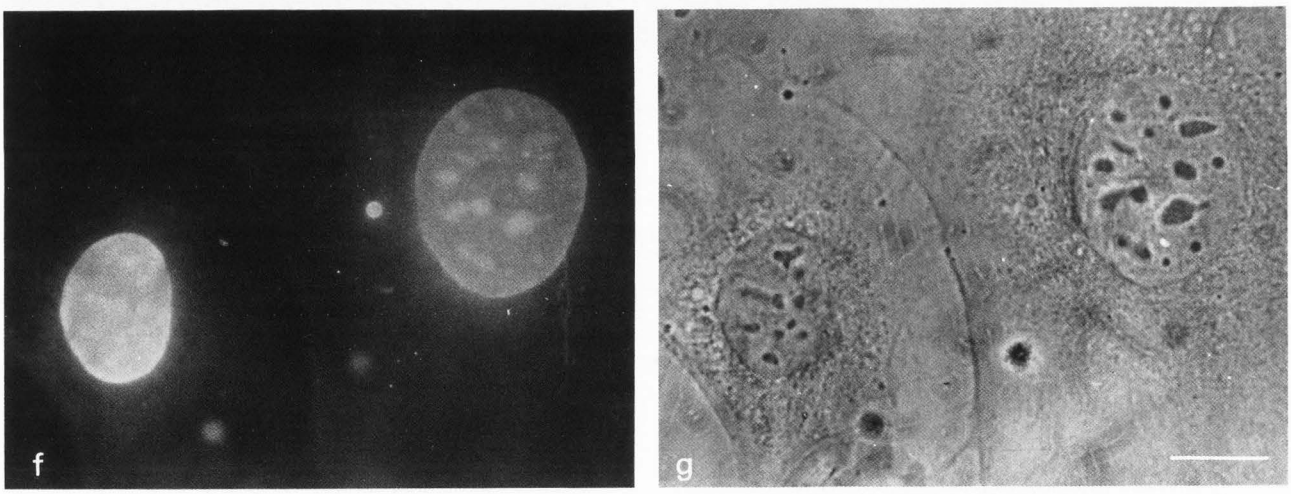

Figs. 4f and g show, for comparison, the image of similar cells imaged by conventional fluorescence and phase contrast microscopy, respectively. Bar = 10 µm.

viewing line. The stereoscopic viewing angles as specified by the values s_1 and s_2 can be chosen to present optimally a certain structure, as arrays of images may be generated for various values of s_1 and s_2 to give an integral picture of the 3-dimensional structure. Stereoscopic imaging in confocal microscopy has also been presented by Carlsson et al. (1985) and Boyde (1985).

Results

Fig. 3 shows the response of the system in reflection to a small object. The measured width of 190 nm is in between the value expected in classical microscopy of 223 nm and 159 nm expected in the confocal case. The classical value was calculated at the indicated conditions with the help of the well-known relation $r = 0.61 \lambda / N.A.$ (r is the width of the response and λ the wavelength). The confocal value following the method indicated in Brakenhoff et al. (1979). That

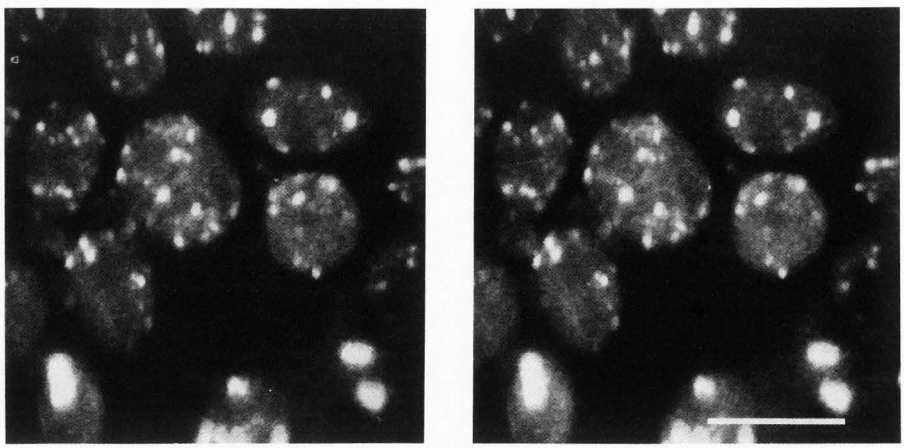

Fig. 5. A high resolution stereoscopic image pair of the actin distribution in the yeast Saccharomyces cerevisiae, stained by phalloidin. Resolution elements down to about 200 nm can be discerned. The images were generated from 13 serial sections taken 0.55 µm apart with the indicated stereoscopic routine, retaining the maximum along the line of sight. Bar = 5 µm.

the response width does not go down to the theoretical confocal value is due to the combined influence of the finite sizes both of the test object and the detector pinhole. Unfortunately, we were not able to measure the response in fluorescence directly due to bleaching and signal-to-noise problems, because of the small amount of radiation emitted by a sufficiently small object. However, results obtained on fluorescent line patterns (reported elsewhere) indicate that the reflection response is a measure for the fluorescent response. From measurements on the same line object we determined that the response along the optical axis (depth resolution of the optical sectioning) under typical conditions (excitation at λ = 480 nm, fluorescence detection around λ = 530 nm) has a width of about 720 nm. This axial response is in good agreement with the result obtained by Wijnaendts van Resandt (1985). For the transverse response width, we found by the same approach a value of 0.2 µm. A fact that is implicitly confirmed by the apparent resolution in the following high-magnification biological images.

The sectioning capability of the instrument is demonstrated in Fig. 4. As can be noted, object elements in the various sections taken 0.65 µm apart are imaged completely independent from each other and do not contribute to adjacent image planes. For comparison we give the images of a comparable specimen as imaged by conventional fluorescence and phase contrast microscopy. An important biological conclusion concerning the structure of the imaged object is that the distribution of nuclear antigen is approximately over a half open sphere coinciding with the periphery of the nucleus, with the open end towards the glass slide on which the cell was grown.

Fig. 5 shows the high resolution spatial capabilities of the instrument on the actin distribution in Saccharomyces cerevisiae yeast cells. Image details down to 200 nm can be discerned. The actin is a component of the cytoskeleton and plays a role in determining the cell shape.

The depth capability of the instrument is demonstrated in the stereoscopical views of the water/fat emulsion mayonnaise in Fig. 6. The total depth range of the views presented is 50 µm. The actual depth range in confocal microscopy is determined in practice by the absorption characteristics of the object. In dense structures, like butter or margarine, it is difficult to obtain an image from a depth beyond 10 µm. In very transparent objects like, for instance, live plant material we have been able to visualize structures beyond 100 µm. The limitations indicated are for high resolution work with N.A. = 1.3 immersion optics.

While in conventional microscopy one can only obtain images in a plane transverse to the optical axis, we can make, with the computer facilities in the CSLM, cross sections along the optical axis. Fig. 6c shows 8 such cross sections, cut at close intervals through the stack of optical sections, put together one above the other in one image. In this set of cross sections one can follow the structure of the cellular fat matrix through the substance very nicely. The quality of a single image from deep in the stack can be judged from Fig. 6d.

The computer-controlled spectroscopic element permits one to visualize structures separately when fluorescing in different wavelength bands. As an example we show in Fig. 7 the separate visualization of the chloroplast and the nuclear DNA material in the algae Closterium moniliferum. Finally in Fig. 8 the use of gold beads as markers in reflection is demonstrated. The location of the gold beads within this thick section of tissue can be very well discerned. The combination of gold beads plus reflection imaging has the advantage over fluorescing probes that often a much stronger signal is acquired, while also no bleaching effects occur.

Comments and Conclusions

Above we have presented some results of confocal microscopy as applied to three-dimensional imaging. A great virtue of the technique is that, once the apparatus is available, it is relatively easy to use and gives fast results. In contrast, techniques based on standard methods in light microscopy involve many operations: sectioning (if thick material is to be studied), photographing the object at various levels, digitizing the images, aligning the images, etc., before 3-D processing can begin. In addition, a type of iterative preprocessing may be necessary to improve the quality of the starting images by compensating for the influence of neighbouring object

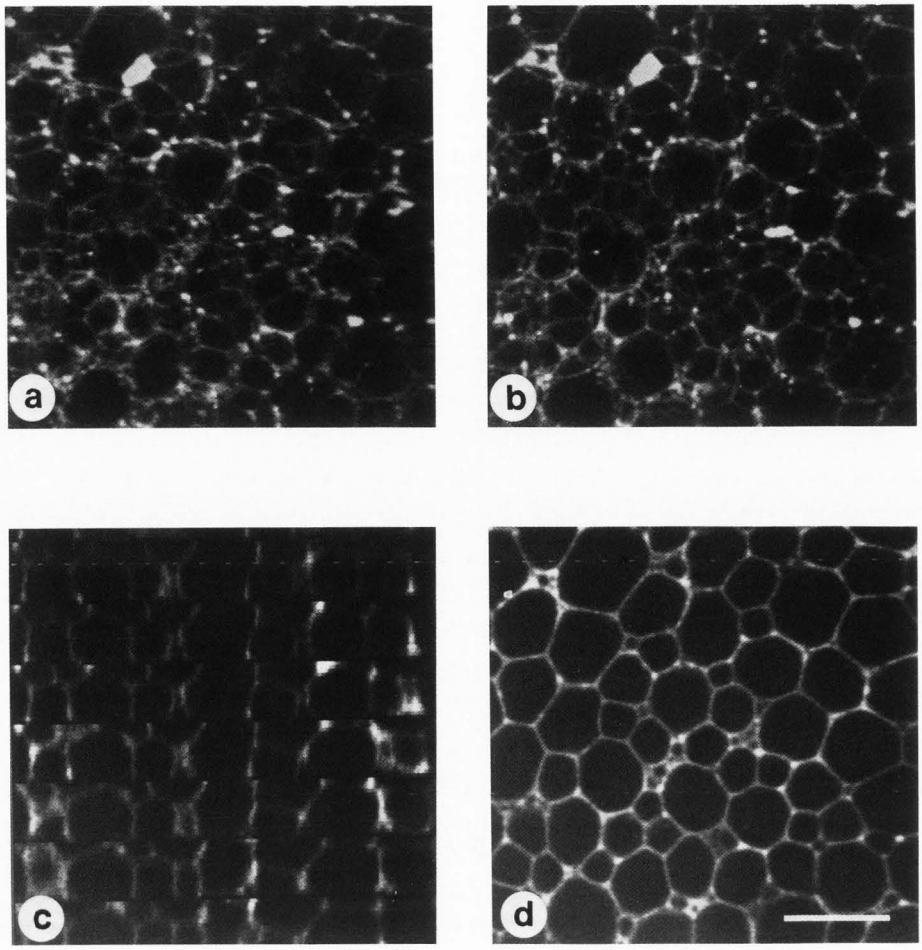

Figs. 6 a, b. Stereoscopic image pair of the 3-D structure of mayonnaise. Visible is the fluorescent network of Nile Blue, dissolved in water, surrounding dark-looking globules with the fat components. The images are constructed from 16 sections 3.2 μm apart, taking the maximum along the sight line. Fig. 6c shows a series of 8 transverse cuts close to each other (see text) through the stack of optical sections while 6d presents one of the sections from which these images were constructed. Bar = 30 μm.

planes (Agard and Sedat, 1983). A comparable situation exists if electron microscopy is used where, in addition, a large number of thin sections must be cut. The latter technique is of course necessary if very high resolutions are required, but if the improved imaging properties of confocal microscopy suffice, a tool has become available that can produce 3-D images in a few minutes. The results presented were all based on sections digitized on a 256 x 256 raster. Collecting the data from one section takes 5 seconds (longer if noise if reduced by averaging) so that with the newly added processing facility (see below) a stereoscopic view, based on 10 sections, can be produced in about one minute.

Very promising for the study of structural organization of multiple cell components is the use of different markers within the specimen. With the present day immunolabelling techniques, highly specific markers for certain proteins, etc., can be developed and then coupled to specific fluorochromes or gold beads. Then, by a combination of 3-D data sets taken in reflection and fluorescence at different wavelengths, we can build up an integrated image representing the spatial organization of the various substances in the specimen. Use of colour in the stereoscopic images will be useful to identify the respective structures.

Future developments will be partly to facilitate an even easier and more effective use of the instrument by the user. With the addition of a new system based on a fast 68020 32-bit processor, it has recently become possible to present the stereoscopic image to the user a few seconds after acquisition of the image data. This makes it possible to use the 3-D information directly for specimen evaluation. However, we think that the main development of the instrument will be in the utilization of the 3-D data sets for image quantification and image analysis. Often specific software will be needed per type of specimen, in order to identify and quantify the desired biological structures and substances. The system recently added is therefore organized so that specific processing algorithms can be incorporated very easily into the system, if necessary written by the user himself in a high level language like Pascal.

In the above we think that we have demonstrated the power and versatility of 3-dimensional imaging based on the confocal optical principle coupled to a computer system. As the examples given indicate, there is a broad field of application in biology and food-structural studies. We expect that the various properties presented above, especially ease of use, will make confocal microscopy in the form we

Figs. 7 a and b show a stereoscopical image pair with fluorescent detection band set by the spectroscopic element in the range of 600-650 nm, while Figs 7 c. and d. show the same object with a detection band of 525-575 nm. Fluorescence exitation at λ = 413 nm. Pair (a, b) is from the same location in the object as pair (c, d). The object is the algae Closterium moniliferum and its chloroplast (pair a, b) is imaged by autofluorescence of the photo synthetic pigments inside, while fluorescence of the nucleus (pair c, d) is due to the vital DNA stain DAPI. Bar = 10 μm.

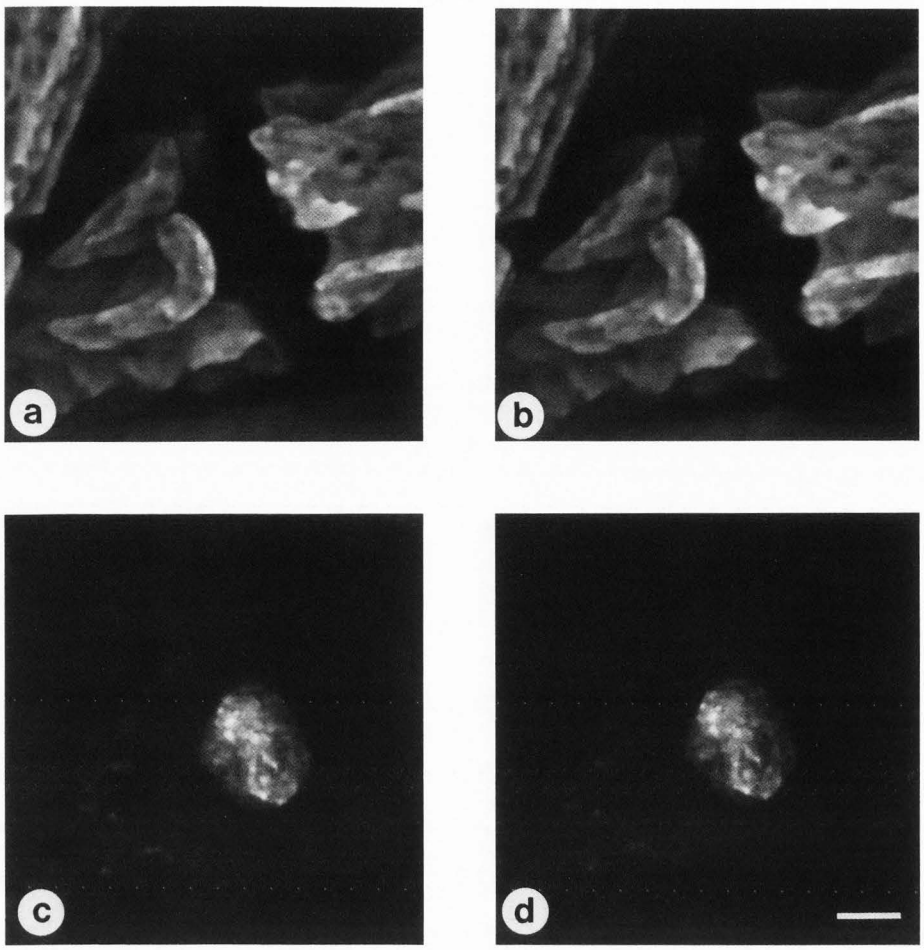

Fig. 8. A stereoscopic image pair of a 10 μm thick section of an embedded rat embryo. In this section the endocytotic vacuoles are marked by small (12 nm) gold beads. In this reflection image, the gold beads, or clusters of them, show up as small high intensity spots, while the more diffuse scattering of the tissue material forms a lower intensity, but still visible background. Bar = 10 μm.

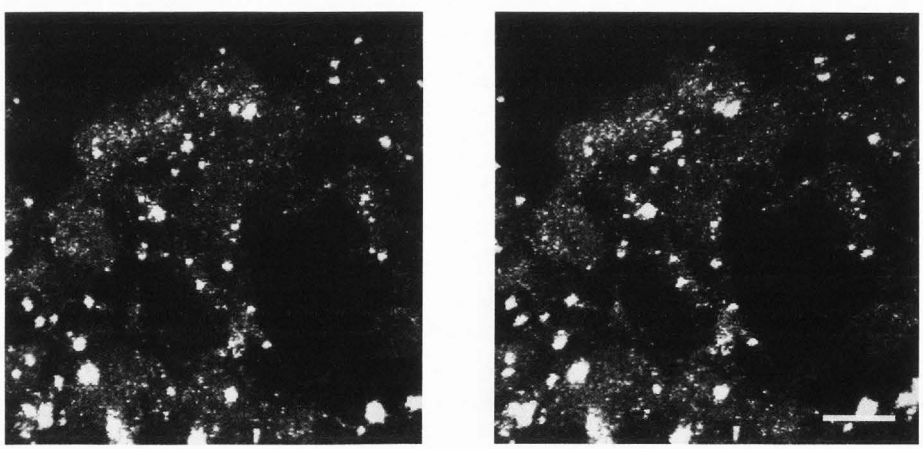

have discussed an important tool for study of the spatial organization of specimens from those fields.

Acknowledgements

We kindly thank R. van Driel, R.E. Poelman and W. de Jong for providing specimen. We are indebted to F.A. Aalst, C. Baarslag and J.A.W. Kalwij for technical assistance. This development was supported by Stichting voor de Technische Wetenschappen (STW) and by the Foundation for Fundamental Biological Research (BION) which is subsidized by the Netherlands Organization for the Advancement of Pure Research (ZWO).

References

Agard DA, Sedat JW (1983) Three-dimensional architecture of a polytene nucleus. Nature 302: 676-681.

Boyde A (1985) Stereoscopic images in confocal (tandem scanning) microscopy. Science 230: 1270-1272.

Brakenhoff GJ, Blom P, Barends P (1979) Confocal scanning light microscopy with high aperture immersion lenses. J. of Microsc. 117: 219-232.

Brakenhoff GJ, Binnerts JS, Barends P (1981) High resolution confocal scanning light microscopy (CSLM) as applied to living biological specimens. Scanning Electron Microsc. 1981; II: 131-138.

Brakenhoff GJ, Van der Voort HTM, Van Spronsen EA, Linnemans WAM, Nanninga N (1985) Three-dimensional chromatin distribution in neuroblastoma nuclei shown by confocal scanning laser microscopy. Nature 317: 748-749.

Carlsson K, Danielson PE, Lenz R, Liljeborg A, Majlöf L, Aslund N (1985) Three-dimensional microscopy using a confocal scanning laser microscope. Opt. Lett. 10: 53-55.

Cox IJ, Sheppard CJR, Wilson T (1982) Super resolution by confocal fluorescence microscopy. Optik 66: 391-396.

Marsman HJB, Stricker R, Wijnaendts van Resandt RW, Brakenhoff GJ (1983) Mechanical scan system for biological applications. Rev. Sci. Instrum. 54: 1047-1052.

Petran M, Hadravsky N, Boyde A (1985) The Tandem Scanning Reflected Light Microscope. Scanning 7: 97-106.

Sheppard CJR, Choudhury A (1977) Image formation in the scanning microscope. Opt. Acta 24: 1051-1073.

Van der Voort HTM, Brakenhoff GJ, Valkenburg JAC, Nanninga N (1985) Design and use of a computer-controlled confocal microscope. Scanning 7: 66-78.

Wijnaendts van Resandt RW (1985) Optical fluorescence microscopy in three dimensions: microtomoscopy. J. Microsc. 138: 29-34.

Woldringh CL, de Jong MA, van den Berg W, Koppes L (1976) Morphological analysis of the division cycle of two Escherichia coli substrains during slow growth. J. Bacteriol. 131: 270-279.

Discussion with reviewers

G. Albrecht-Buehler: How does the system deal with the algorithm generated by cover-glass embedding medium, etc? How much does astigmatism influence the resolution?
Authors: Due to the fact that nearly the whole light path from objective lens to object is in media of refractive index with a value of (or very close to) n = 1.515 (i.e., immersion oil and carrier glass), we do not expect any astigmatism from these causes as the immersion lenses used are designed for operation under those conditions. Only when traversing an embedded specimen, having a different refractive index, one may expect some influence. The limitations for this were indicated in Brakenhoff et al. (1981) In practice, we see that with our high N.A. system, we do not find an appreciable reduction of resolution up to penetration depths in the specimen of 20-30 µm. A distance sufficient for examination at full resolution of the 3-dimensional structure of many biological preparations. At greater depths (we have worked up to depths of 100-150 µm) a gradually increasing loss of detail is discerned.

G. Albrecht-Buehler: What is the size of the mechanical distortions of the mechanical scanning device? Does the electronic display correct them?
Authors: No effort has been made to correct these distortions, although technically possible, by electronic means. The distortions within the image are limited to about 5%. The response measurements were calibrated for a specific condition with the help of calibration replica with 463 nm line spacing.

A.Boyde: What is the limit of sensitivity for your type of microscope?
Authors: In confocal microscopy the effective imaging properties are a product of the illumination conditions and the detection conditions. Now in on-axis confocal microscopy, the illumination distribution can be made very close to optimal, as one can work with very small illumination pinholes. Due to the used laser light sources, always sufficient illumination intensity can be produced. In the detection step of the generated reflection or fluorescence radiation one can choose in on-axis and in off-axis scanning, but not in Tandem Reflection Microscopy, the specific size of pinhole for the result desired. Optimal resolution can be realized with a small pinhole with as a penalty low signal collection efficiency. If no sufficient signal is available, one can employ a somewhat larger pinhole. We have noted that resolution both lateral and axial is only marginally affected for pinhole sizes up to half the measure of the Rayleigh resolution, projected in the detection plane. The sensitivity of the instrument is determined by the above-mentioned aspects; the quantum efficiency of the detectors used (in our case S-20 response photomultipliers) and of course the transmission properties of the optical elements. The limits of sensitivity are finally determined by the overall quantum efficiency of the system.

C.J.R. Sheppard: Are all the stereo pairs produced by processing 10 planes of data? Is there a limit to the number of planes you can handle? How many pixels are there in the axial section of Fig. 6 c?
Authors: No, the stereo pairs are produced by processing varying numbers of data planes. In the images shown, it varies between 6 and 16. The limit in the number of data planes is basically unlimited, data are stored on disc plane by plane. In practice more than 16 slices are hardly ever necessary. In fig. 6c there are 16 pixels in the axial direction.

C.J.R. Sheppard: What is the application of assigning a minimum value along a viewing line?
Authors: The idea behind this facility is that in this way one can visualize "holes" inside otherwise solid structures not readily visible with either the maximum or summation routine.